

Article

Impacts of Climate Change and Human Activity on the Runoff Changes in the Guishui River Basin

Meilin Wang ¹, Yaqi Shao ¹, Qun'ou Jiang ^{1,2,3,*}, Ling Xiao ^{1,2}, Haiming Yan ⁴, Xiaowei Gao ⁵, Lijun Wang ⁵ and Peibin Liu ⁵

¹ School of Soil and Water Conservation, Beijing Forestry University, Beijing 100083, China; merlin902@bjfu.edu.cn (M.W.); syqheim1014@bjfu.edu.cn (Y.S.); xiaoling@bjfu.edu.cn (L.X.)

² Key Laboratory of Soil and Water Conservation and Desertification Prevention, Beijing Forestry University, Beijing 100083, China

³ Jinyun Forest Ecosystem Research Station, School of Soil and Water Conservation, Beijing Forestry University, Beijing 100083, China

⁴ School of Land Resources and Urban & Rural Planning, Digital Territory Experiment Center, Hebei GEO University, Shijiazhuang 050031, China; haiming.yan@hgu.edu.cn

⁵ Beijing Institute of Water, Beijing 100048, China; gaoxiaowei@biwmail.com (X.G.); Wanglijun@biwmail.com (L.W.); Liupeibin@biwmail.com (P.L.)

* Correspondence: jiangqo@bjfu.edu.cn; Tel.: +86-1581-077-8541

Received: 25 July 2020; Accepted: 21 August 2020; Published: 23 August 2020



Abstract: Guishui River Basin in northwestern Beijing has ecological significance and will be one of the venues of the upcoming Beijing Winter Olympic Games in 2022. However, accelerating climate change and human disturbance in recent decades has posed an increasing challenge to the sustainable use of water in the basin. This study simulated the runoff of the Guishui River Basin using the Soil and Water Assessment Tool (SWAT) model to reveal the spatio-temporal variations of runoff in the basin and the impacts of climate change and human activities on the runoff changes. The results showed that annual runoff from 2004 to 2018 was relatively small, with an uneven intra-annual runoff distribution. The seasonal trends in runoff showed a decreasing trend in spring and winter while an increasing trend in summer and autumn. There was a first increasing and then decreasing trend of average annual runoff depth from northwest to southeast in the study area. In addition, the contributions of climate change and human activities to changes in runoff of the Guishui River Basin were 60% and 40%, respectively, but with opposite effects. The results can contribute to the rational utilization of water resources in the Guishui River Basin.

Keywords: SWAT model; runoff changes; climate change; human activities; Guishui River Basin

1. Introduction

Water resources are key to human survival and development and form an integral component of ecosystems. However, water resources at a global scale are facing increasing threats due to rapid economic development, population growth, and urban expansion [1]. Climate change has changed the temporal and spatial distribution of global precipitation, temperature and other meteorological elements, resulting in an increase in the frequency and intensity of floods and droughts [2]. It is predicted that by 2025, 3 billion people will have insufficient access to potable water, and 40 countries and regions will be water stressed [3]. China, as the world's most populous country, hosts approximately 18% of the global population (1.4 billion people), but with only 6% of global freshwater resources. China therefore faces long-term challenges related to water deficits and an uneven spatial and temporal distribution of water resources [4–6]. In recent years, water stress in China has been exacerbated by the deterioration of the ecological environment, and by the use of outdated and water inefficiency

technology in industry and agriculture, serious waste of water, and water pollution; thereby, seriously limiting national economic development in China [7,8]. Therefore, obtaining further knowledge on the impact of the changing environment on water resources is essential for achieving sustainable development of water resources [9].

The current dominant drivers of change to the environment that significantly affect water resources include climate change and human activities [10,11]. Climate change, in particular precipitation, is the driving factor of spatial and temporal changes to water resources [12]. The accelerating impacts of global warming have resulted in water management authorities globally placing increasing focus on simulation methods of water resources [13]. The United Kingdom issued the "White Paper on Water Policy-Water for Life", which proposed comprehensive reforms in the water intake permit system, water industry, environmental management, and water conservation to ensure water security and the ecological integrity of aquatic ecosystems. China has similarly responded to the challenge posed to water resources by climate change through various means, including strengthening water resources infrastructure and improving water resource allocation [14,15]. However, the significant impact of human activities on water resources must also be considered [16]. There has been a move by countries globally to move towards a stage of "new urbanization" since the beginning of the 20th century. The rapid development of agriculture and industry coinciding with rapid increases in human populations have seen a gradual increase in the impacts of human activities on water resources [17]. Water deficits which are exacerbated by water pollution are becoming increasingly prevalent, and water is therefore increasingly becoming a major limiting factor to economic development of a basin [18,19]. Nash et al. found that climate change is the leading factor leading to the change of runoff in the Colorado River Basin [20]. Bewket et al. believed that the leading factor for change in runoff is man-made destruction of the natural environment [21]. Current researches treat human activities and climate change as two non-interfering factors, and assess their impact on runoff changes by separating their impact on the hydrological process of the basin. However, how to correctly separate the effects of climate change from human activities is still quite difficult.

Hydrological modeling remains the primary means of exploring and understanding the complex hydrological processes of a river basin, which can be categorized into lumped or distributed models [22]. Lumped hydrological models operate at the entire basin; therefore, they do not consider the spatial heterogeneity of hydrological elements, and variables and parameters used in the model are mostly averaged. In contrast, distributed hydrological models discretize the watershed into smaller spatial units; thereby, considering surface and subsurface flow changes at a finer spatial scale, so as to more accurately reflect the true hydrological process in the watershed [23]. With the continuous development of remote sensing and geographic information system technology, the Soil and Water Assessment Tool (SWAT) model, which is equipped with an ArcGIS (geographic information system) platform, has been widely used in hydrological simulation studies [24–26].

The Guishui River Basin is located in the Yanqing District of Beijing and will be one of the venues for the 2022 Winter Olympic Games. Since the availability of water and snow in the mountainous area of the basin will be essential for the success of the games, there will be increasing focus on developing a rational and sustainable water management policy for the basin. However, Beijing has suffered droughts lasting nearly 10 years since the beginning of the late 20th century. Affected by the terrain of the Guichuan Basin, the average annual precipitation in the Guishui River Basin is generally low. Guishui River traverses the Guichuan Basin and is surrounded by mountains on three sides. Due to the closed topography of the basin and the surrounding mountains, it is difficult for the ocean water vapor to enter and there is little precipitation. Therefore, the precipitation supply of Guishui River becomes less. In addition, large-scale production and construction activities accompanying economic development have led to a sharp drop in the runoff into the Guishui River Basin, which has led to increasing water deficits; thereby, restricting the regional ecological environment, social and economic harmony, and sustainable development. Therefore, the present study applied the SWAT model to simulate the runoff of the Guishui River Basin in the Yanqing District of Beijing. This allowed the

analysis of the temporal and spatial variations of runoff in the basin. On this basis, the present study attempted to distinguish between the relative contributions of climate change and human activities to changes of the runoff in the Guishui River, with a view to providing a scientific basis for the rational planning and management of water resources in the Guishui River Basin.

2. Materials and Methods

2.1. Study Area

The Guishui River Basin is located with an area of 625.83 km² in the northwest of Beijing (40°21′50″–40°38′40″ N and 115°48′51″–116°20′42″ E), and includes the towns of Zhangshanying, Jiuxian, Xiangying, Liubinbao, Yongning, and Jingzhuang (Figure 1). The northern, eastern, and southern sides of the basin are surrounded by high mountains, whereas the central part is flat with a small number of hilly areas, mainly composed of low-lying wetlands, lakeside plain, and alluvial plain near the river banks. The Guishui River Basin is situated adjacent to the Guanting Reservoir in the West. The study area has a typical continental monsoon climate in the northern temperate zone, with cold and dry winters and cool and rainy summers. According to meteorological data from 1990 to 2018, the annual average temperature is 10 °C and the average yearly precipitation is ~466 mm. Moreover, the rainy season extends from June to September, accounting for 70%–80% of annual rainfall. The main sources of water in the basin are precipitation, groundwater and releases from the Baihebu Reservoir. Surface water in the basin accounts for 16.2% of the total surface water resources in the Yanqing District, and the distribution of groundwater resources is relatively uneven. In recent years, the river flow has declined due to the gradual increase in household and industrial water consumption. In addition, there has been increasing over-exploitation of groundwater resources. Therefore, there are increasingly prevalent and severe periods of water deficit in the basin.

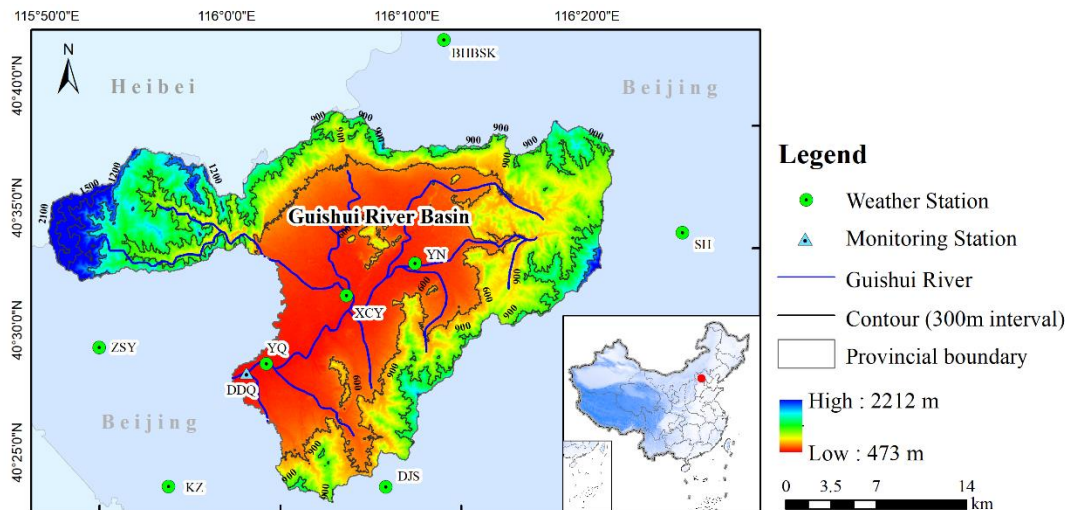


Figure 1. Location of study area.

2.2. Data Sources and Processing

The datasets used in this study included meteorological, hydrological, land use, digital elevation model (DEM), and soil data. Daily meteorological data for the period 2004–2018 were obtained from the Beijing Meteorological Bureau of the Yanqing District and the China Meteorological Data Network, covering eight stations including the Baihebu Reservoir, Zhangshanying, Xiangcunying, Yongning, Sihai, Kangzhuang, Jiushi, and Yanqing. As there are only three weather stations situated within the study area, data from a further five weather stations situated nearby were used to interpolate meteorological data to a grid scale. Monthly runoff data from 2004 to 2018 were obtained from the

Water Affairs Bureau of Yanqing District, Beijing, which were for a monitoring station at the control section of the East Bridge in Yanqing District.

The land use data in 2008 and 2018 were obtained based on the Système Probatoire d'Observation de la Terre (SPOT) remote sensing images through manual visual interpretation. The spatial resolutions of the remote sensing images were 1.5 m × 1.5 m. Interpretation of the land use data of 2018 was verified based on field surveys, with a verification accuracy of 96.5%. Land use data was reclassified and recoded into a total of 7 categories according to the SWAT land use classification system: (1) cultivated land (AGRL), (2) forestry area (FRST), (3) orchard land (ORCD), (4) grassland (HAY), (5) water area (WATR), (6) built-up area (URHD), and (7) barren land (BARR).

The DEM data were downloaded from the Advanced Spaceborne Thermal Emission and Reflection Radiometer Global Digital Elevation Model (ASTER GDEM) dataset provided by the geospatial data cloud, with a spatial resolution of 30 m × 30 m. The soil type distribution map was derived from the spatial distribution data of the soil types of China provided by the resource and environment data cloud platform, with a spatial resolution of 1 km × 1 km. The general parameter values of some soil properties were derived from Volume 4 of the Chinese Soil Species and the Chinese Soil Database.

2.3. Methodology

2.3.1. SWAT Model

The SWAT model, developed by the Agricultural Research Center of the US Department of Agriculture, is a physically-distributed hydrological model applied at the watershed scale [27,28]. Hydrological simulation in the SWAT model mainly involves two parts. The first is the land phase of the hydrological cycle following the water balance principle (Equation (1)), and includes precipitation, runoff, evapotranspiration, infiltration, and backflow components [29]. This process regulates the input of water, sediment, and nutrients from the main channels in each sub-basin. The second part is the confluence stage of the hydrological cycle, which mainly involves the confluence calculation of the main river channel and the reservoir [30]. This stage simulates the migration of water, sediment, and other substances from the river channel to the watershed outlet.

$$SW_t = SW_0 + \sum_{i=1}^t (R_{day} - Q_{surf} - E_a - W_{seep} - Q_{gw}) \quad (1)$$

In Equation (1), SW_t is the final soil water content (mm), SW_0 is the initial soil water content on day i (mm), R_{day} is precipitation on day i (mm), Q_{surf} is surface runoff on day i (mm), E_a is evapotranspiration on day i (mm), W_{seep} is the amount of water entering the aeration zone from the soil profile on day i (mm), Q_{gw} refers to the returned water volume on day i (mm), and t refers to the time (days).

2.3.2. Runoff Impact Assessment Model

Within the runoff impact assessment model, the hydrological model was used to simulate runoff under the assumption that there is no obvious disturbance during the disturbance period (Figure 2). Therefore, it is necessary to establish the time node of base period and disturbance period [17]. Then, the hydrological model, which was calibrated over the base period, was used to simulate the runoff over the disturbance period so as to quantify the overall impacts of both climate change and human activities on watershed runoff.

The change in observed runoff data between the base period and disturbance period allowed overall change in runoff to be calculated using Equation (2). At the same time, the change in total runoff could be approximated as the sum of runoff changes resulting from climate change and human activities, which can be expressed by Equation (3) [31].

$$\Delta Q = \left| \overline{Q_{o2}} - \overline{Q_{o1}} \right| \quad (2)$$

$$\Delta Q = \Delta Q_c + \Delta Q_h \tag{3}$$

In Equations (2) and (3), ΔQ is the total runoff change, $\overline{Q_{o2}}$ is the average observed runoff during the disturbance period, $\overline{Q_{o1}}$ is the average observed runoff during the base period, and ΔQ_c and ΔQ_h are changes of the runoff resulting from climate change and human activities, respectively.

Based on the SWAT simulations of runoff, ΔQ_c and ΔQ_h could be further expressed by Equations (4) and (5).

$$\Delta Q_c = |\overline{Q_s} - \overline{Q_{o1}}| \tag{4}$$

$$\Delta Q_h = |\Delta Q - \Delta Q_c| \tag{5}$$

In Equation (4), Q_s is the average simulated runoff during the disturbance period.

Furthermore, the relative contributions of climate change and human activities to changes of the river basin runoff could be expressed by Equations (6) and (7), respectively.

$$\mu_c = \frac{\Delta Q_c}{|\Delta Q_c| + |\Delta Q_h|} \times 100\% \tag{6}$$

$$\mu_h = \frac{\Delta Q_h}{|\Delta Q_c| + |\Delta Q_h|} \times 100\% \tag{7}$$

In Equations (6) and (7), μ_c and μ_h represent the contributions of climate change and human activities to changes of the runoff in the basin, respectively.

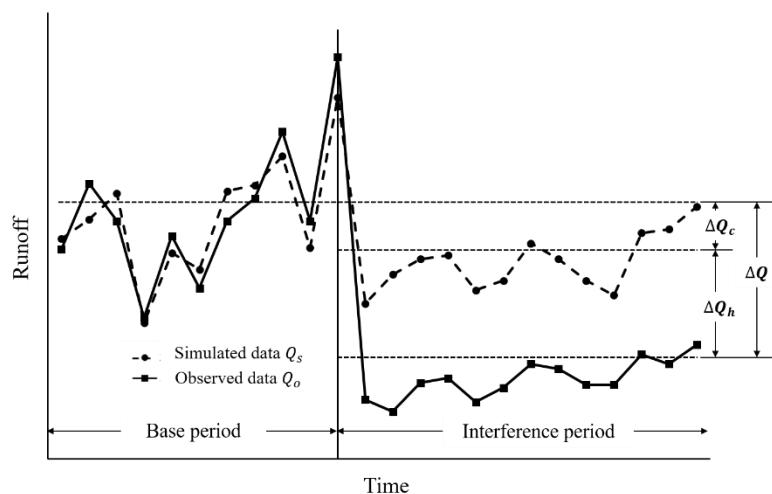


Figure 2. Runoff impact assessment model.

2.3.3. The Runoff-Concentration Degree and Runoff-Concentration Period

The runoff-concentration degree (RCD) and runoff-concentration period (RCP) are important indicators to reflect the concentration of annual runoff and the period of maximum runoff with monthly runoff. The RCD refers to the proportion of the combined amount of the horizontal and vertical components of the monthly runoff in the annual runoff, and reflects the concentration of the annual runoff during the year. The RCP represents the orientation of the runoff vector after synthesis, and reflects the date when the center of gravity of the runoff concentration during the year appears. They can be expressed by the following formula:

$$R_x = \sum_{i=1}^{12} r_i \sin \theta_i, R_y = \sum_{i=1}^{12} r_i \cos \theta_i \tag{8}$$

$$RCD = \frac{\sqrt{R_x^2 + R_y^2}}{R} \quad (9)$$

$$RCP = \arctan \frac{R_x}{R_y} \quad (10)$$

where R is the annual runoff; R_x and R_y represent the horizontal and vertical components formed by the sum of the components of 12 months ($i = 1, 2, 3, \dots, 12$), respectively.

2.4. Calibration and Verification of the SWAT Model

This study ensured maximum accuracy of the simulated results by applying the SWAT calibration and uncertainty analysis tool SWAT Calibration and Uncertainty Procedures (SWAT-CUP) and the continuous uncertainty matching algorithm Sequential Uncertainty Fitting Version 2 (SUFI-2), developed by the Swiss Federal Institute of Aquatic Sciences [32]. These procedures were used for a model sensitivity analysis and a subsequent model calibration and verification. The results of parameter sensitivity by the SUFI-2 algorithm was evaluated by the t -stat statistic, with larger absolute values of t -stat indicating greater influence of a particular parameter on model simulations. The p -value is used to determine the significance of the influence, with p -value closer to 0 indicating greater significance. It is reasonable to assume that the SWAT model parameters would be sensitive to the flood and non-flood seasons; therefore, the model was separately calibrated and verified for the two seasons in this study. Since the flood season of the Guishui River Basin generally extends from June to September, this study applied June to September as the flood season and October to May of the following year as the non-flood season. Table 1 showed the results of global sensitivity analysis of the parameters after setting the initial range of the parameters and performing 1500 simulations for the flood and non-flood seasons.

Table 1. The sort of the sensitive parameters.

Period	Rank	Parameters	Definition	t -Stat	p -Value
Flood season	1	SOL_K	Saturated hydraulic conductivity	16.07	0.00
	2	CANMX	Maximum canopy storage	6.52	0.00
	3	CN2	SCS runoff curve number	2.38	0.02
	4	SLSUBBSN	Average slope length	2.15	0.03
	5	ESCO	Soil evaporation compensation factor	−1.91	0.06
	6	GW_REVAP	Groundwater "revap" coefficient	1.56	0.12
	7	HRU_SLP	Average slope steepness	−1.44	0.15
	8	CH_K1	Effective hydraulic conductivity in tributary channel alluvium	1.28	0.20
	9	CH_N2	Manning's "n" value for the main channel	1.25	0.21
	10	ALPHA_BF	Baseflow alpha factor	−0.94	0.35
Non-flood season	1	GWQMN	Threshold depth of water in the shallow aquifer required for return flow to occur	11.39	0.00
	2	SOL_AWC	Available water capacity of the soil layer	4.14	0.00
	3	CANMX	Maximum canopy storage	2.56	0.01
	4	ESCO	Soil evaporation compensation factor	−2.11	0.04
	5	HRU_SLP	Average slope steepness	−1.89	0.06
	6	GW_DELAY	Groundwater delay	−1.57	0.12
	7	RCHRG_DP	Deep aquifer percolation fraction	−1.57	0.12
	8	CH_K1	Effective hydraulic conductivity in tributary channel alluvium	−1.54	0.13
	9	SFTMP	Snowfall temperature	−1.47	0.14
	10	SURLAG	Surface runoff lag time	1.32	0.19

A preliminary investigation found that the period of 2004–2011 was characterized by relatively minor influence of human activities on water resources in the Guishui River Basin, and therefore the

basic model was constructed on data from this period. The periods 2004–2005, 2006–2008, and 2009–2011 were set as the model warm-up, calibration, and verification periods, respectively, of which data for January to April were only available for 2011. The determination coefficient (R^2), the Nash–Sutcliffe efficiency coefficient (NSE), and the percentage deviation (P_{BIAS}) [33] were used to evaluate model performance in addition to visual fits by comparing plots of observed verses simulated data at the watershed outlet. On the basis of the model performance evaluation criteria adopted in previous studies, simulation results can be considered reasonable when $NSE > 0.50$, $R^2 > 0.50$, and P_{BIAS} is within $\pm 25\%$ [34]. For a more detailed description of the evaluation criteria, please refer to Moriasi et al. (2007) [35].

During the flood season, SWAT simulations (Table 2) obtained R^2 values larger than 0.6 during both the calibration and verification periods. The NSE values obtained over the calibration and verification periods were 0.77 and 0.62, respectively, whereas those of P_{BIAS} were within $\pm 25\%$ for both periods. These results indicated a good correlation between the model simulation and observation data. The mean simulated runoff during the calibration period (Figure 3) was a little higher than that of the observed runoff over the entire period, but the accuracy of the simulated results was still acceptable. In contrast, the mean simulated runoff over the verification period was slightly smaller than that of the observed runoff. Comparative speaking, the simulated results for the verification period were slightly better than those over the calibration period, and the relative error between the simulated and observed data was 1%.

Table 2. Accuracy evaluation of simulated results by the Soil and Water Assessment Tool (SWAT) model.

		Evaluation Index			Runoff Characteristics(m ³ /s)	
		R ²	NSE	P _{BIAS}	Simulated Mean	Observed Mean
Flood season	Calibration period	0.78	0.77	−2.1	0.275	0.269
	Validation period	0.68	0.62	1	0.130	0.132
Non-flood season	Calibration period	0.64	0.62	1.4	0.289	0.293
	Validation period	0.68	0.52	−0.4	0.324	0.323

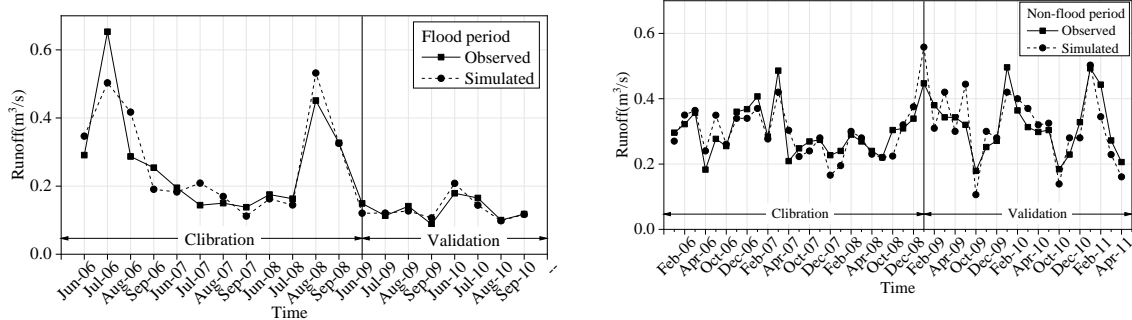


Figure 3. Comparison between simulated value and observed value in different periods.

During the non-flood season, the model simulations achieved R^2 larger than 0.6 for both the calibration and verification periods. The NSE values of model simulations over the calibration and verification periods were 0.62 and 0.52, respectively, whereas P_{BIAS} over both periods were within $\pm 25\%$. The relative errors of runoff simulation for both periods were relatively small, at 1.4% and -0.4% , respectively. In general, these results indicated good correlation between simulated and observed data, although the model performance was not as good as that for the flood season.

3. Results

3.1. Spatio-Temporal Evolution of the Runoff in the Guishui River Basin Under a Changing Environment

3.1.1. Interannual Variations and Spatial Distribution of the Runoff in the Guishui River Basin

A statistical analysis on the runoff over time for the Guishui River Basin showed there were a generally small annual runoff averaging $0.11 \times 10^8 \text{ m}^3$ (Figure 4). This can be attributed to the temperate and semi-arid continental climate of the Guishui River Basin, with less precipitation compared to other regions of Beijing. Annual runoff showed an insignificant increasing trend of $0.06 \times 10^8 \text{ m}^3 10 \text{ a}^{-1}$. The largest and smallest annual runoff was for 2018 and 2014 at $0.37 \times 10^8 \text{ m}^3$ and $0.04 \times 10^8 \text{ m}^3$, respectively. There was a gentle downward trend before 2012 with $-0.10 \times 10^8 \text{ m}^3 10 \text{ a}^{-1}$ followed by a fluctuating but overall positive trend, but a particularly steep increase over 2017–2018, with an average increase over 2012–2018 of $0.39 \times 10^8 \text{ m}^3 10 \text{ a}^{-1}$, close to four times as that of the decline period. This can be explained by the conversion of some barren land or grassland to forestry area over the period 2004–2011, resulting in a decline in runoff to some extent. In contrast, the Baihebao Reservoir supplied additional water to the Guishui River after this period.

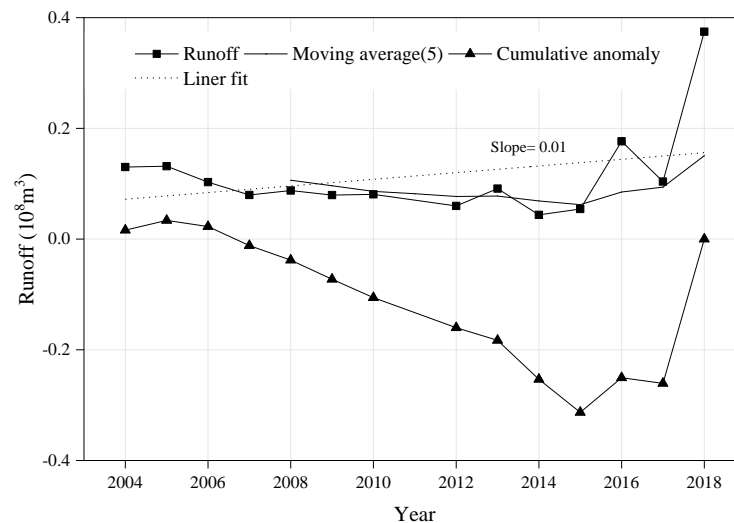


Figure 4. Runoff changing trend in the Dongdaqiao station from 2004 to 2018.

The SWAT simulations of sub-basin runoff depth were used to explore the spatial distribution of sub-basin runoff (Figure 5). The distribution of average runoff depth in the sub-basin from 2006 to 2011 showed that there were an initial increase and then a decrease from northwest to southeast in the study area. The average runoff depth was relatively small at 3.85 mm. Sub-basins producing larger runoff depths were concentrated in the central region, with a maximum runoff depth of 38.2 mm appearing in the central No. 24 sub-basin, which was also the outlet of the watershed. Runoff depths generated at sub-basins along the watershed edge were relatively smaller, with the minimum runoff depth of 0.13 mm appearing in the No. 3 sub-basin in the northwest mountainous area of the basin. A spatial overlay of runoff depth with land use area ratio (Figure 5a–e) and DEM data (Figure 5f) showed that runoff depths generated in sub-basins containing large areas of cultivated land and built-up area were relatively large. This could be due to the cultivated land and built-up areas being located in the plain areas in the central basin, which were the areas where water accumulates. In additionally, this region has a large impervious surface area, characterized by decreased rainfall interception and infiltration. The sub-basin containing a large area of forestry area in the upstream mountainous area had a smaller runoff depth, which can be explained by the smaller water storage capacity of the tributary and the stronger water interception function of forest vegetation. In addition, the relationship between the

area ratio of orchard land or grassland and runoff depth was not clear, possibly because the scattered distributions of grassland and orchard land in the region compared to the other three land use types.

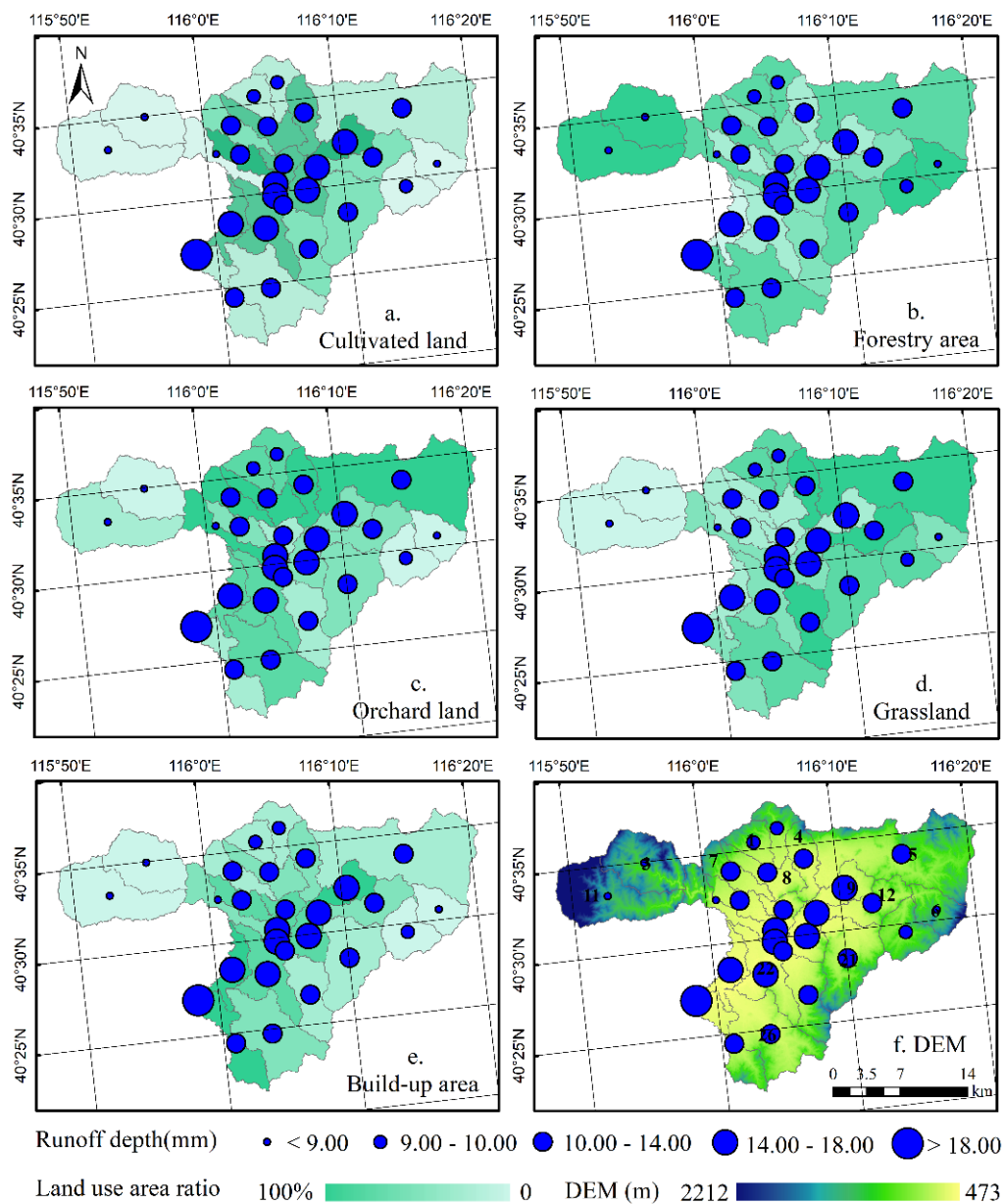


Figure 5. Spatial distribution of annual average runoff depth in the Guishui River Basin.

3.1.2. Seasonal Variations of the Runoff in the Guishui River Basin

The seasonal variation of runoff in the Guishui River Basin was analyzed by categorizing runoff over March to May, June to August, September to November, and December to February as spring, summer, autumn, and winter runoff, respectively. Seasonal fluctuations in runoff were evident (Figure 6). Average runoff in spring was $0.02 \times 10^8 \text{ m}^3$, with an overall downward trend. The maximum and minimum runoffs appeared in 2005 and 2016, respectively. Runoff trends over winter were similar to that over spring, with an evident decreasing trend. Average annual runoff in winter was $0.03 \times 10^8 \text{ m}^3$, slightly higher than that over spring. In contrast, an increasing trend in autumn runoff was evident, with an average runoff of $0.03 \times 10^8 \text{ m}^3$, with the maximum occurring in 2018. The runoff in autumn was relative higher during the period of 2012–2018 due to the water release from Baihebu

Reservoir in this season. Summer runoff similarly showed an overall increasing trend, with a multi-year average runoff of $0.04 \times 10^8 \text{ m}^3$.

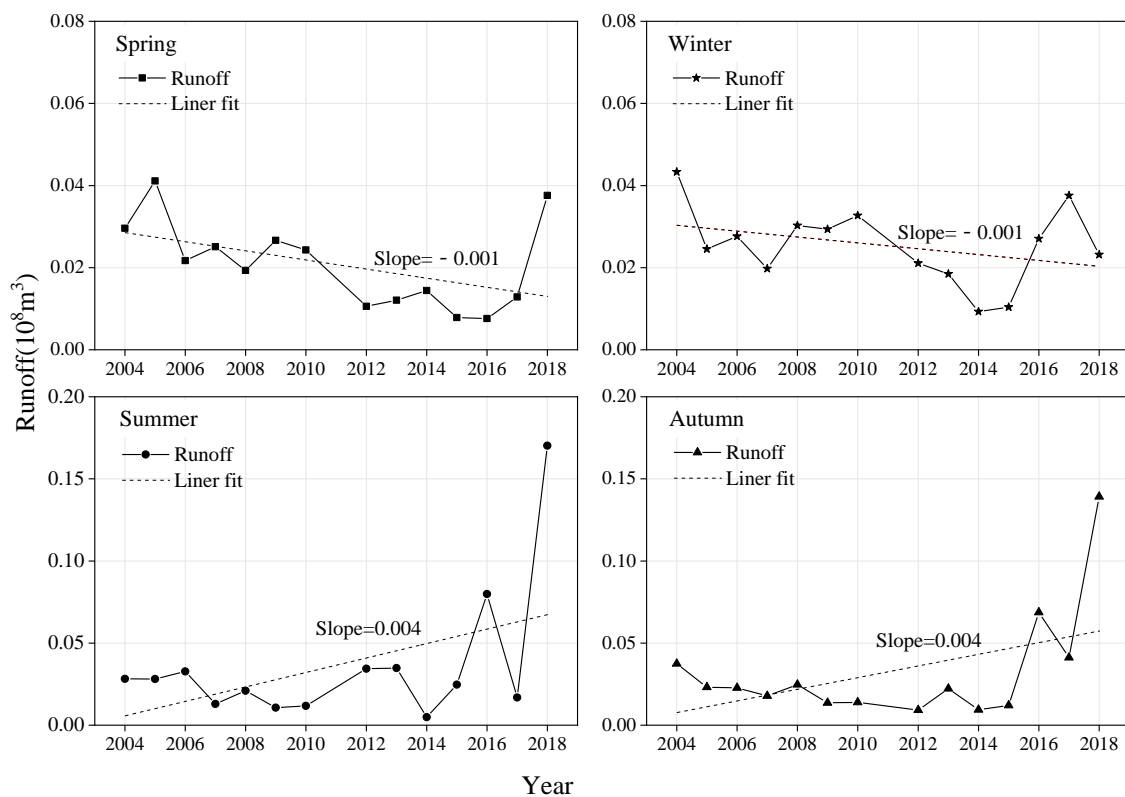


Figure 6. Seasonal runoff changing trend in the Dongdaqiao station from 2004 to 2018.

An analysis of the spatial variation in runoff depth over different seasons at the sub-basin scale (Figure 7) identified seasonal trends that were different to those of runoff to some extent. This observation may be due to water transfer from other basins or through water interception. In general, the spatial distributions of runoff depth in the sub-basins were similar for spring, summer, and autumn, with a common pattern of greater runoff depths in the central area and less in the surrounding area on the northern, eastern, and southeast sides. The spatial distribution of runoff depth in winter showed that it was greater within the region extending from the middle to the perimeter of the basin, encompassing the sub-basins located in the mountainous areas on both sides of the northern and southern basin. This can be explained by the melting of snow and ice in the mountain area at the end of winter and early spring, resulting in increased runoff in the sub-basins in these areas. To be specific, the overall runoff of each sub-basin in spring was small, with an average runoff depth of 0.6 mm. In contrast, the runoff in each sub-basin increased significantly in summer due to increased precipitation, particularly in sub-basins located in the central flat area. Although the runoff of each sub-basin in autumn was similar to that in summer, the average runoff depth was only 0.3 mm. This observation may be due to less precipitation in autumn. Winter runoff in the mountainous sub-basins increased due to the freeze–thaw process, with an average runoff depth of 1.0 mm.

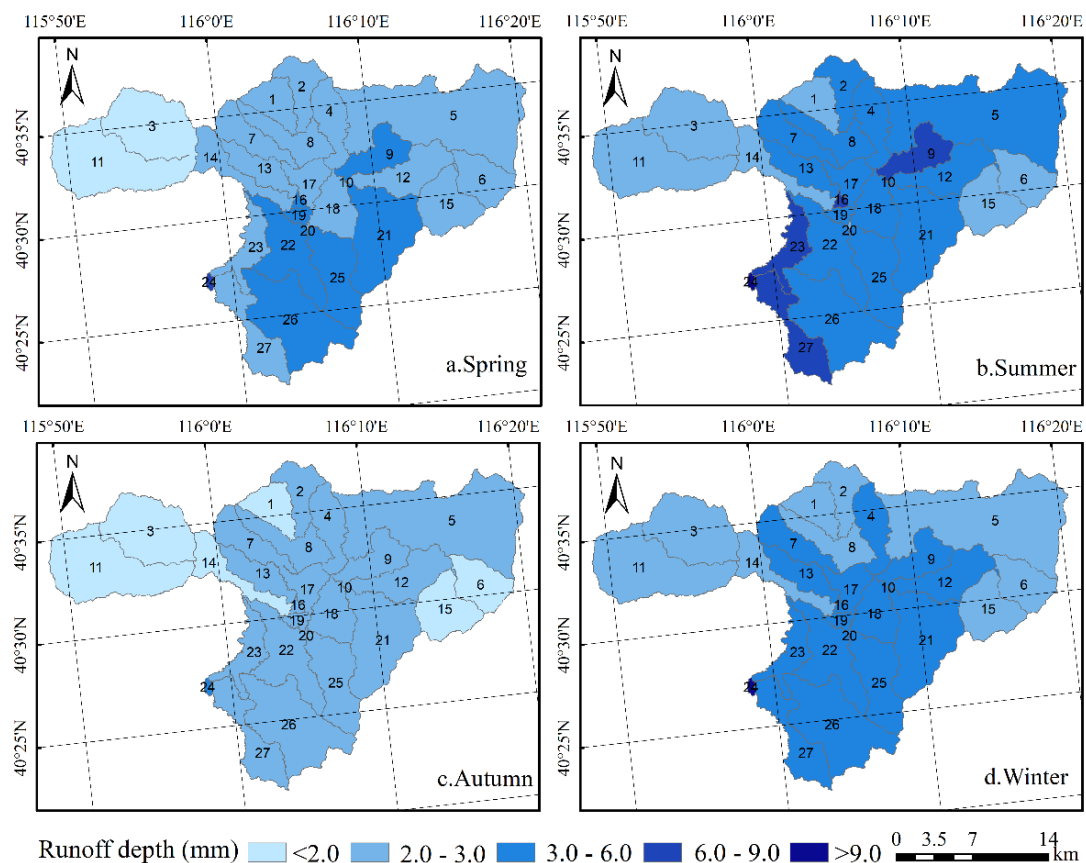


Figure 7. Spatial distribution of seasonal runoff depth in the Guishui River Basin.

3.1.3. Intra-annual Variation of the Runoff in the Guishui River Basin

The runoff-concentration degree (RCD) and runoff-concentration period (RCP) indicators were applied to represent the intra-annual distribution of runoff in the Guishui River Basin during the period of 2004–2018 (Figure 8). The results showed an uneven intra-annual distribution of runoff in the Guishui River Basin. The average annual runoff in the basin from 2004 to 2018 was $0.01 \times 10^8 \text{ m}^3$, with the maximum and minimum occurring in August and June at $0.019 \times 10^8 \text{ m}^3$ and $0.005 \times 10^8 \text{ m}^3$, respectively. Runoff concentration over the study period averaged 0.29, with the highest and lowest runoff concentrations occurring in 2018 and 2006 at 0.56 and 0.04, respectively. One-dimensional linear fitting on the concentration and concentration period series from 2004 to 2018 showed that the runoff concentration increased overall. The runoff concentration period fluctuated around 17 July, with the period before 2012 mostly occurring in middle and late May, whereas it was delayed after 2012. This observation can be explained by an increase in precipitation in the basin after 2012 as well as replenishment of the upstream reservoirs and other human activities. Runoff in the basin began to concentrate in the flood season under the influence of climate change and human activities.

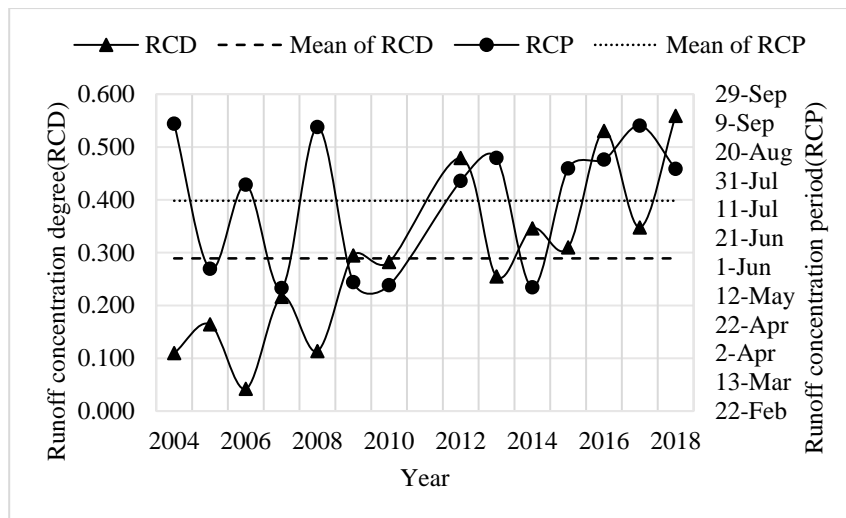


Figure 8. Runoff-concentration degree/period in the Dongdaqiao station from 2004 to 2018.

3.2. Impact of Climate Change and Human Activities on the Runoff in the Guishui River Basin

3.2.1. Identification and Evaluation of the Factors Influencing the Runoff in the Guishui River Basin

Climate change and human activities will have a variety of annual impacts on runoff in the basin, so this study used the average value of runoff representing the runoff level during one period. This study used the period 2006–2011 as the base period, and then analyzed the impact of climate change and human activities on the runoff in the Guishui River Basin by comparing runoff over the period 2012–2018 with that over the base period. Because there was a large inter-annual variation of runoff, the average runoff over 2006–2011 was used as the base runoff for comparison, following which the year in which the runoff was close to the baseline over the period 2006–2011 was identified. At the same time, the land use data in the identified year was used as the baseline for land use over the baseline period. It was assumed that land use did not change over the base period of 2006–2011, whereas there was a change in climate from 2012 to 2018. The calibrated SWAT model was then used to simulate the runoff under the influence of climate change over the period 2012–2018. The actual observed runoff from 2012 to 2018 was then used to minus the simulated runoff under the influence of climate change, whose results was regarded as the change caused by the impact of human activities. The relative contributions of climate change and human activities to changes in the runoff were then estimated (Figure 9).

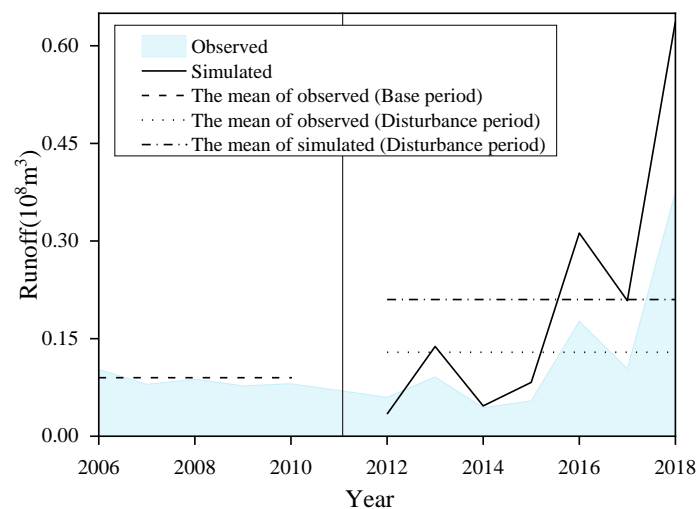


Figure 9. Runoff impact assessment model results in the Guishui River Basin.

Mean observed annual runoff during the period 2012–2018 was $0.13 \times 10^8 \text{ m}^3$, which was higher than that during the period of 2006–2011 at $0.09 \times 10^8 \text{ m}^3$, with an evident increasing trend. Therefore, the total change in runoff ΔQ was $0.04 \times 10^8 \text{ m}^3$, which included the combined effects of climate change and human activities. Mean simulated annual runoff for the period 2012–2018 was $0.21 \times 10^8 \text{ m}^3$. It was proposed that the change of the runoff due to climate change was $0.12 \times 10^8 \text{ m}^3$, whereas that due to human activities was $-0.08 \times 10^8 \text{ m}^3$. It indicated that when there was only the impact of climate change, the runoff would show an increasing trend, while when there was only the impact of human activity, the runoff would show a decreasing trend. In addition, this study explored the impact of land use change by replacing the land use data with that in 2018 while keeping the remaining input data unchanged. The results showed that changes of runoff due only to land use change was $-0.01 \times 10^8 \text{ m}^3$. It was found that the relative contributions of climate change and human activities to changes of the runoff in the Guishui River Basin were 60% and 40%, respectively. Among which, the contribution of the land use change was 5%. Climate change led to an increase in runoff, while human activities promoted runoff decrease. Therefore, it was clear that both climate change and human activities had a significant impact on the runoff of the Guishui River Basin, their impacts were opposing, and the contribution rate of climate change was slightly greater than that of human activities, which was consistent with the research results of Yuliang Zhou.

3.2.2. Impact of Climate Change on the Runoff in the Guishui River Basin

Changes of the runoff in the Guishui River Basin were the result of a combination of various climatic factors. However, due to the available meteorological data being limited to a town level, this study only analyzed the impact of climate change on the runoff of the Guishui River Basin in terms of precipitation and temperature.

Correlation Analysis between Precipitation and Runoff

The Pearson correlation coefficient was used to analyze the correlation between runoff and precipitation at annual and seasonal scales (Figure 10). At the intra-annual scale, the correlation between monthly means of runoff and precipitation had a coefficient R of 0.47 ($P > 0.1$), indicating a certain correlation and synchronization between the runoff and precipitation in the river basin. Jia et al. (2014) also found the seasonal and inter-annual variability of precipitation was a major cause of uncertainty [36]. The seasonal-scale analysis found that the correlation coefficients R between precipitation and runoff in spring, summer, autumn, and winter were 0.29 ($P > 0.1$), 0.40 ($P > 0.1$), -0.32 ($P > 0.1$) and 0.23 ($P > 0.1$), respectively, indicating positive correlations between precipitation and runoff in spring, summer, and winter, but a negative correlation in autumn. However, the R coefficients indicated low correlations in summer and autumn but no significant correlation in spring and winter. This result was also an indication of the complexity of factors affecting the runoff in the Guishui River Basin. In addition to precipitation, human activities were also important factors affecting the runoff. In addition, regardless of the season being summer or autumn, moderate precipitation corresponded with increased runoff in 2018. The observed data indicated that the Baihebu Reservoir had released 29 million cubic meters into the Guishui River to ensure the quality of the water during the World Expo in 2018. During this time, released water in summer and autumn exceeded 77% of the total runoff. Therefore, an outlier relationship between runoff and precipitation appeared in the summer and autumn of 2018. Cheng et al. (2019) analyzed the characteristics of precipitation changes by using the meteorological data of Yanqing National Basic Weather Station from 1960 to 2018. During the last six decades, there was a significant decrease in annual precipitation and the rate was $-4 \text{ mm}/10\text{a}$. Years with more and less precipitation appeared alternately in a wave shape. Zhang et al. (2017) counted the precipitation data of Yanqing Station in Beijing from 1999 to 2016 and found that the level of precipitation in Yanqing area was the highest in June, and the precipitation was the highest in July. They all increased first and then decreased from January to December.

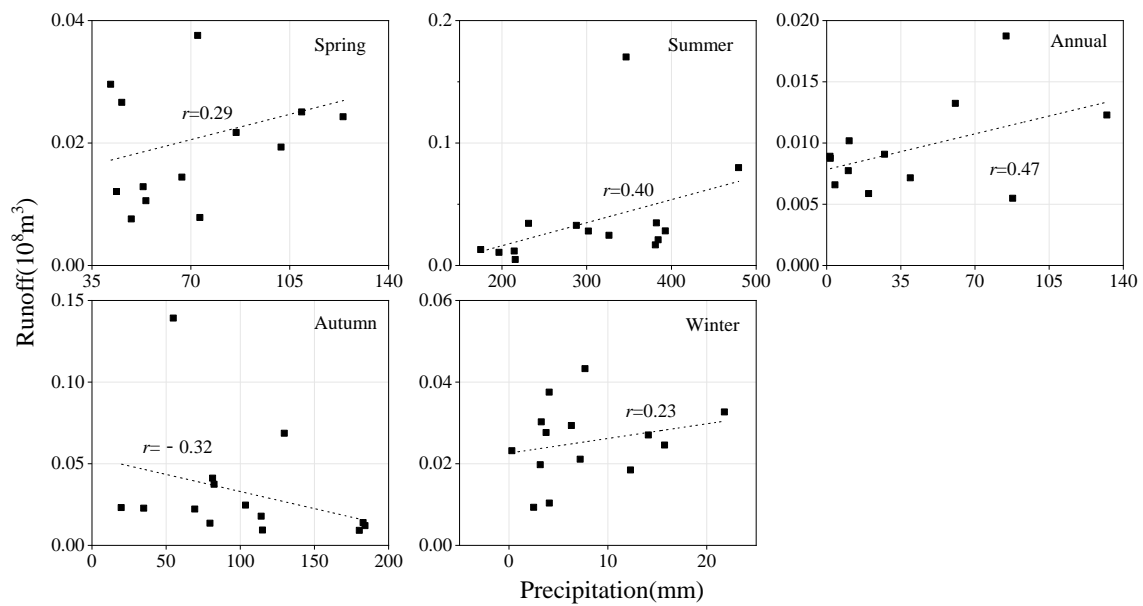


Figure 10. Correlation between runoff and precipitation at annual and seasonal scales.

Correlation Analysis between Temperature and Runoff

The Pearson correlation coefficient was also used to explore the correlation between temperature and runoff at annual and seasonal scales (Figure 11). A weak positive correlation between annual mean temperature and annual runoff was identified with a correlation coefficient R of 0.37 ($P > 0.1$). At the seasonal scale, a moderately positive correlation was identified between mean temperature and runoff in summer, with a correlation coefficient of 0.54 ($P > 0.1$). However, negative correlations between mean temperature and runoff were identified in spring, autumn, and winter, but the correlations in spring and autumn were not significant. These results indicated that the impact of temperature on runoff was obvious mainly in summer, due mainly to additional rain and heat occurring in the same period in the Guishui River Basin. Yang et al. (2011) found that the increase in runoff lost to evaporation could be as high 3.8 mm with a temperature rise of 1 °C in the Yixun River basin [37].

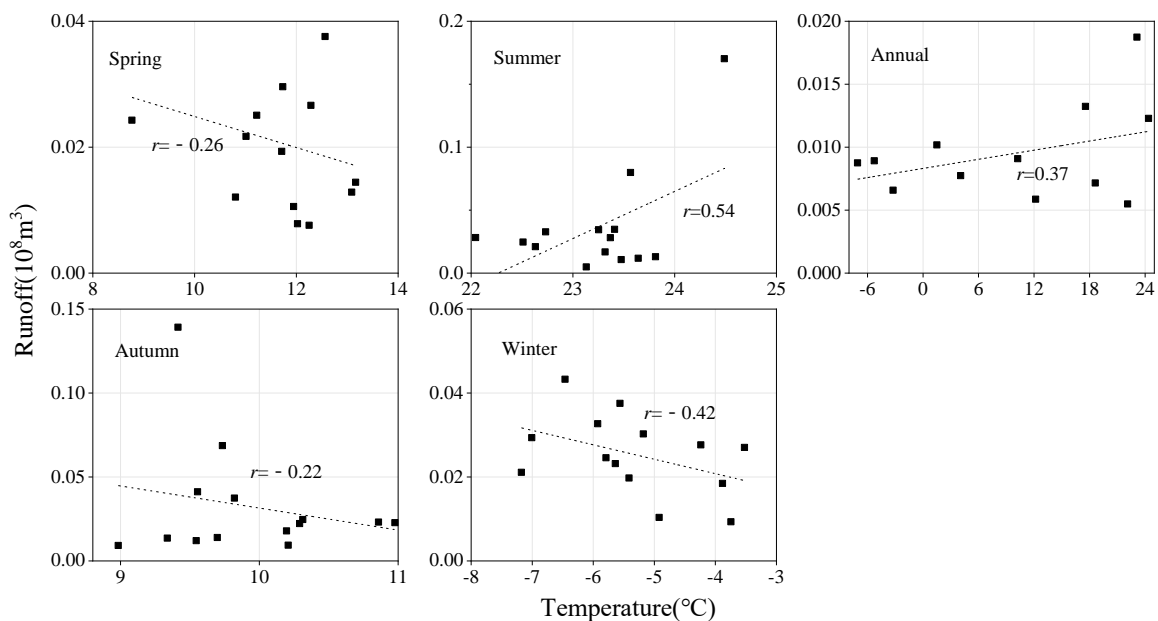


Figure 11. Correlation between mean temperature and runoff at annual and seasonal scales.

3.2.3. Impact of Human Activities on the Runoff in the Guishui River Basin

There were many factors involved in the impact of human activities on runoff of the Guishui River Basin, including land use change, water supply in the basin and social and economic development. However, since it was not easy to separate the impact of each factor, this study analyzed only the impact of land use change on runoff of the Guishui River Basin.

Spatial-Temporal Variation of Land Use in the Guishui River Basin

Using land use data in the Guishui River Basin, this study explored the changes of land use spatial patterns in the basin (Figure 12). The results showed that there were relatively large areas of cultivated land and forestry area accounting for 27.68% and 53.03%, respectively. This result was consistent with that was found by Jie (2016) [38]. Forestry area was mainly distributed in the mountainous areas along the northern and southern sides of the basin, whereas cultivated land was concentrated in the central plain areas and at the feet of the mountains. These land uses were concentrated spatially. Orchard land was mainly distributed between cultivated land areas, accounting for 2.51% of the total area. Grassland was mostly distributed along the border between cultivated land and forestry area, accounting for 8% of the total area. Built-up area was scattered between cultivated lands or near the rivers. During the study period, the area of forestry area in the Guishui River Basin increased by 5.99%, whereas those of built-up area and barren land also showed an increasing trend, with increases of 2.78% and 1.15%, respectively. This observation may be due to the implementation of many projects such as the Winter Olympics and World Expo, which had damaged the ecological environment of the area to a certain extent. In contrast to the land use types mentioned above, there were continuous declines in the areas of cultivated land, orchard land, grassland, and water area of 3.60%, 1.88%, 4.32%, and 0.12%, respectively, possibly related to recent urbanization. The increasing population and the accompanying expansion of urban areas have led to conversion of some basic ecological land such as cultivated land, orchard land, and grassland to urban built-up area.

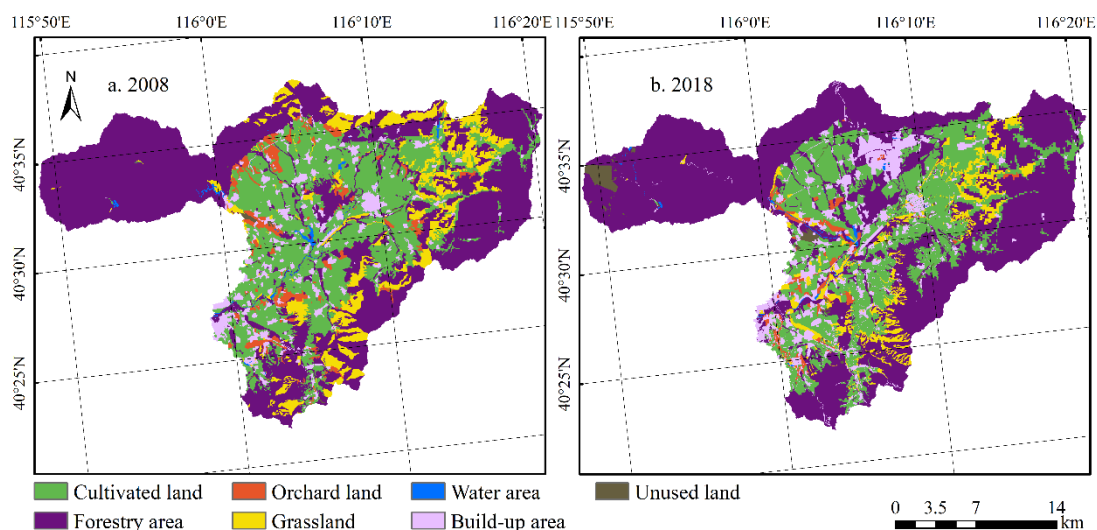


Figure 12. Spatial distribution of land use in Guishui River Basin in 2008 and 2018.

Impacts of Land Use Change on the runoff in the Guishui River Basin

The runoff impact assessment showed that the contribution of land use change to runoff reduction in the Guishui River Basin was 5% (Figure 13). As seen from the spatial distribution of runoff change, land use change in most of the sub-basins resulted in reduced runoff, especially in the area surrounding the Guishui River Basin. On one hand, large-scale afforestation in the rock mountain area was expected to have increased runoff interception and infiltration capacity, whereas the Guishui River Basin was located in the ecotone between a sub-humid and sub-arid climate. Since the beginning of the early

21st century, the Yanqing District Government had successively implemented ecological restoration projects such as tree planting and afforestation, returning farmland to forestry area to control erosion and improve the environmental health of ecologically fragile areas in the basin [39]. As of 2018, more than 300,000 acres of afforestation in the barren hills has been achieved. The introduction of vegetation guaranteed not only an improved water conservation function, but also effectively reduced the slope runoff [40]. This was mainly because the vegetation canopy can intercept and redistribute precipitation, the surface vegetation layer and litter layer can slow down or block runoff flow, and then water conservation capacity increased, which also reduced the runoff to a certain extent.

In addition, the expansion of urban area in the basin has often been accompanied by population growth and social and economic development [38]. The 2018 statistical yearbook of the Yanqing District listed the permanent population of the region to have been 348,000 at the end of 2018, which was very close to the lower threshold of the regional population carrying capacity based on the total amount of water resources in the region [41], and 80% of the population resided in the Guishui River Basin. Furthermore, the Guishui River Basin had become a major agricultural production area and was also becoming an important industrial area with the continuous adjustment of the industrial structure of Yanqing District. The town of Yongning was the economic and trade center of the eastern part of the river basin, with agriculture and agricultural product processing forming the core development industries [42]. The majority of economic activity occurring in the remaining towns located in the river basin was related to tourism and agriculture. Under this context of population distribution and economic development, water deficits in the river basin have become increasingly severe, leading to a continuous increase in surface water and groundwater extraction in the basin. The groundwater level has seen continuous yearly declines [43]. The ecological base flow of the Guishui River can therefore not be effectively guaranteed, the runoff of the river has been further attenuated and some sections of the river have even experienced periods of no flow.

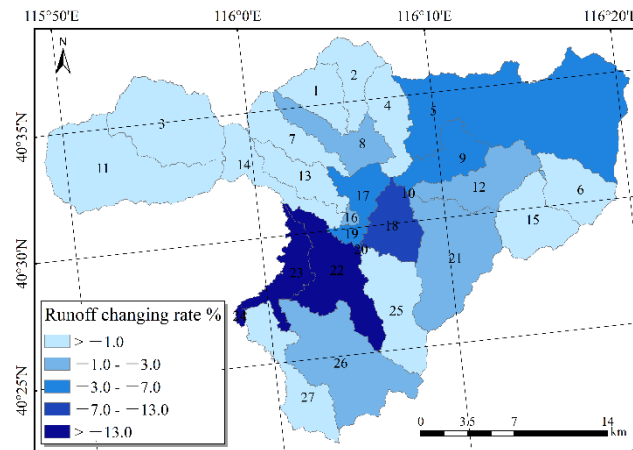


Figure 13. Contribution of land use change to runoff in each sub-basin.

4. Discussion

Firstly, since agriculture in the Guishui River Basin has very high water demands, the implementation of water-saving irrigation technology can play a decisive role in the reduction of water use [44]. However, currently only about 10% of total irrigation area employed the water-saving irrigation technology. Therefore, it is recommended that the local government should accelerate the construction of water-saving irrigation technology, such as precision irrigation, sprinkler irrigation, and drip irrigation [5]. At the same time, management of irrigation systems can be improved through the use of technology such as moisture sensors to automatically adjust irrigation schedules based on soil moisture. In addition, farmers generally lack awareness of the importance of conserving water as farmers have traditionally paid very little for water, which led to the phenomenon of wastage. Therefore, it is recommended that the Yanqing District Government speed up the implementation of the

water charge system in rural area to offer incentives for the effective implementation of water-saving agriculture [45].

The recycling of water is an additional approach to conserving water in the basin. At present, most irrigation water for agriculture in the Guishui River Basin was extracted from groundwater, surface water, and water storage facilities, and the contribution of recycled water remains relatively minor [46]. At the same time, aquaculture ponds of varying sizes existed in the watershed, which pose a threat to the water quantity and quality of the watershed. Therefore, it is suggested that the local government implement the "Cultivation and Aquaculture Cycle" model based on the development of ecologically sustainable agriculture in the Guishui River Basin. Microbial treatment technology can be applied to reprocess water from the aquaculture ponds for the use as agricultural irrigation water [11]. Such agricultural circulation systems have already been successfully implemented in countries like Israel [47]. The "Cultivation and Aquaculture Cycle" model can not only reduce the extraction of irrigation water from groundwater and surface river to improve the efficiency of recycling water resources, but also can reduce the discharge of contaminated water to rivers and lakes to alleviate water pollution.

Finally, due to the disparities between water supply and demand, which can differ seasonally, and the need to trade-off development with protection of the aquatic environment, it is recommended that relevant departments implement a demand management model [48] for water resources in the river basin to alleviate water deficits and water use conflicts. During periods of high-water deficits, it is recommended to consider adopting an irrigation model that controls the allocation of water to agricultural and forest irrigation. That is, irrigation water could be preferentially allocated to crops or forestry during sensitive stages when sufficient water is imperative, such as during the crop or forestry seedling stages, and measures for reducing irrigation can be adopted during the non-sensitive stages [49]. The premise of this policy implementation is to allow a threshold of water reduction that can nevertheless ensure maximum economic benefit per unit of water volume, so as to alleviate conflict between agriculture and forest while conserving water resources.

5. Conclusions

In this study, a calibrated and verified SWAT model was used to estimate and analyze the temporal and spatial evolution of runoff for the Guishui River Basin. Although the results showed an overall increasing trend in runoff of the Guishui River Basin under the influence of gradual warming and humidification after 2011, due to limiting human activities, the overall amount of water resources in the basin remained low. Flood control, ecology, tourism, industry, agricultural production, and other human socio-economic development demands are closely intertwined with water resources in the river basin to form a complex "hydro-ecological-economic" ternary structure. The negative impacts of human activities on the water resources of river basins have become increasingly profound. At present, the total demand for water resources for social economic development and ecological protection has exceeded total available water resources in the river basin, resulting in increasing conflict among competing demands. This need is re-enforced by the fact that the success of the upcoming 2022 Winter Olympics depends on the effective management of water resources in the basin. Based on the analysis of the evolution of runoff and the contributing factors in the Guishui River Basin, this study proposes some strategies of managing water resources, including recycling and coordinated management of the river basin, with a view to providing a scientific reference for the rational and sustainable use of water resources in the Guishui River Basin.

Author Contributions: Conceptualization, M.W., Y.S., and Q.J.; methodology, M.W., Y.S., and L.X.; software, M.W., Y.S., and Q.J.; formal analysis, M.W., Y.S., and Q.J.; resources, M.W., Y.S., Q.J., and L.X.; data curation, M.W., Y.S., and Q.J.; writing—original draft preparation, M.W., Y.S., and Q.J.; writing—review and editing, Q.J., H.Y., X.G., L.W., and P.L.; visualization, M.W. and Y.S.; supervision, Q.J.; and funding acquisition, Q.J., X.G., L.W., and P.L. All authors have read and agreed to the published version of the manuscript.

Funding: This project was funded by the National Science and Technology Projects (No.2017ZX07101004 and No. 2017ZX07108002), and the National Natural Science Foundation of China (No. 41901234 and No.51909052).

Acknowledgments: Data provision and support from projects of the National Natural Science Foundation of China (No.71225005) and the Exploratory Forefront Project for the Strategic Science Plan in IGSNRR, CAS are also appreciated. In addition, we gratefully acknowledge the Beijing Municipal Education Commission for their financial support through Innovative Transdisciplinary Program “Ecological Restoration Engineering”.

Conflicts of Interest: The authors declare no conflict of interest.

References

1. Wang, Q.; Xu, Y.P.; Wang, Y.F.; Zhang, Y.Q.; Xiang, J.; Xu, Y.; Wang, J. Individual and combined impacts of future land-use and climate conditions on extreme hydrological events in a representative basin of the Yangtze River Delta; China. *Atmos. Res.* **2020**, *236*. [[CrossRef](#)]
2. Peng, H.; Jia, Y.W.; Qiu, Y.Q.; Niu, C.W.; Ding, X.Y. Assessing climate change impacts on the ecohydrology of the Jinghe River basin in the Loess Plateau, China. *Hydrol. Sci. J.* **2013**, *58*, 651–670. [[CrossRef](#)]
3. Piyush, D.; Madan, L.S.; Jeeban, P.; Dhiraj, P. Modeling the future impacts of climate change on water availability in the Karnali River Basin of Nepal Himalaya. *Environ. Res.* **2020**, *185*. [[CrossRef](#)]
4. Zhou, Y.L. Quantitative evaluation of the impact of climate change and human activity on runoff change in the Dongjiang River Basin; China. *Water* **2018**, *10*, 571. [[CrossRef](#)]
5. Chu, H.B.; Wei, J.H.; Qiu, J.; Li, Q.; Wang, G.Q. Identification of the impact of climate change and human activities on rainfall-runoff relationship variation in the Three-River Headwaters region. *Ecol. Ind.* **2019**, *106*. [[CrossRef](#)]
6. Huo, A.D.; Wang, X.F.; Cheng, Y.X.; Zheng, C.L. Impact of future climate change (2020–2059) on the hydrological regime in the heihe river basin in shanxi province; China. *Int. J. Big Data Min. Glob. Warm.* **2019**, *1*, 1950003. [[CrossRef](#)]
7. Guo, S.S.; Zhu, Z.R.; Lyu, L. Effects of climate change and human activities on soil erosion in the Xihe River Basin; China. *Water* **2018**, *10*, 1085. [[CrossRef](#)]
8. Qiu, J.L.; Shen, Z.Y.; Hou, X.S.; Xie, H.; Leng, G.Y. Evaluating the performance of conservation practices under climate change scenarios in the Miyun Reservoir Watershed; China. *Ecol. Eng.* **2020**, *143*. [[CrossRef](#)]
9. Sarma, A.K.; Saharia, A.M. Future climate change impact evaluation on hydrologic processes in the Bharalu and Basistha basins using SWAT model. *Nat. Hazards* **2018**, *92*, 1463–1488. [[CrossRef](#)]
10. Jiang, C.; Xiong, L.H.; Wang, D.B.; Liu, P.; Guo, S.L.; Xu, C.Y. Separating the impacts of climate change and human activities on runoff using the Budyko-type equations with time-varying parameters. *J. Hydrol.* **2015**, *522*, 326–338. [[CrossRef](#)]
11. Wang, J.F.; Gao, Y.C.; Wang, S. Assessing the response of runoff to climate change and human activities for a typical basin in the Northern Taihang Mountain; China. *J. Earth Syst. Sci.* **2018**, *127*. [[CrossRef](#)]
12. Abbas, S.A.; Xuan, Y. Impact of precipitation pre-processing methods on hydrological model performance using high-resolution gridded dataset. *Water* **2020**, *12*, 840. [[CrossRef](#)]
13. Hilo, A.N.; Saeed, F.H.; Al-Ansari, N. Impact of climate change on water resources of Dokan Dam Watershed. *Engineering* **2019**, *11*, 464–474. [[CrossRef](#)]
14. Yin, J.; He, F.; Xiong, Y.J.; Qiu, G.Y. Effects of land use/land cover and climate changes on surface runoff in a semi-humid and semi-arid transition zone in northwest China. *Hydrol. Earth Syst. Sci.* **2017**, *21*, 183–196. [[CrossRef](#)]
15. Yang, Q.L.; Luo, S.S.; Wu, H.C.; Wang, G.Q.; Han, D.W.; Lü, H.S.; Shao, J.M. Attribution analysis for runoff change on multiple scales in a humid subtropical basin dominated by forest; east China. *Forests* **2019**, *10*, 184. [[CrossRef](#)]
16. Opp, C.; He, X.; Lotz, T. Factors of runoff generation in the Dongting Lake basin based on a SWAT model and implications of recent land cover change. *Quat. Int.* **2018**, *475*, 54–62. [[CrossRef](#)]
17. Deng, X.Z.; Zhang, F.; Wang, Z.; Li, X.; Zhang, T. An extended input output table compiled for analyzing water demand and consumption at county level in China. *Sustainability* **2014**, *6*, 3301–3320. [[CrossRef](#)]
18. Omer, A.; Wang, W.; Basheer, A.K.; Yong, B. Integrated assessment of the impacts of climate variability and anthropogenic activities on river runoff: A case study in the Hutuo River Basin; China. *Hydrol. Res.* **2017**, *48*, 416–430. [[CrossRef](#)]

19. Dosdogru, F.; Kalin, L.; Wang, R.Y.; Yen, H. Potential impacts of land use/cover and climate changes on ecologically relevant flows. *J. Hydrol.* **2020**, *584*. [[CrossRef](#)]
20. Nash, L.; Gleick, P.H. Sensitivity of streamflow in the Colorado basin to climatic changes. *J. Hydrol.* **1991**, *125*, 221–241. [[CrossRef](#)]
21. Bewket, W.; Sterk, G. Dynamics in land cover and its effect on stream flow in the Chemoga watershed, Blue Nile basin, Ethiopia. *Hydrol. Process. Int. J.* **2005**, *19*, 445–458. [[CrossRef](#)]
22. Koo, H.; Chen, M.; Jakeman, A.J.; Zhang, F.Y. A global sensitivity analysis approach for identifying critical sources of uncertainty in non-identifiable; spatially distributed environmental models: A holistic analysis applied to SWAT for input datasets and model parameters. *Environ. Model. Softw.* **2020**, *127*. [[CrossRef](#)]
23. Miller, S.N.; Baker, T.J. Using the Soil and Water Assessment Tool (SWAT) to assess land use impact on water resources in an East African watershed. *J. Hydrol.* **2013**, *486*, 100–111. [[CrossRef](#)]
24. Jayakrishnan, R.; Srinivasan, R.; Santhi, C.; Arnold, J.G. Advances in the application of the SWAT model for water resources management. *Hydrol. Process.* **2005**, *19*, 749–762. [[CrossRef](#)]
25. Fukunaga, D.C.; Cecilio, R.A.; Zanetti, S.S.; Oliveira, L.T.; Caiado, M.A.C. Application of the SWAT hydrologic model to a tropical watershed at Brazil. *Catena* **2015**, *125*, 206–213. [[CrossRef](#)]
26. Jakada, H.; Chen, Z. An approach to runoff modelling in small karst watersheds using the SWAT model. *Arab. J. Geosci.* **2020**, *13*. [[CrossRef](#)]
27. Yu, Y.D.; Liu, J.H.; Yang, Z.Y.; Cao, Y.Q.; Chang, J.; Mei, C. Effect of climate change on water resources in the Yuanshui River Basin: A SWAT model assessment. *Arab. J. Geosci.* **2018**, *11*, 1–9. [[CrossRef](#)]
28. Hu, J.; Ma, J.; Nie, C.; Xue, L.Q.; Zhang, Y.; Ni, F.Q.; Deng, Y.; Liu, J.S.; Zhou, D.K.; Li, L.H.; et al. Attribution analysis of runoff change in Min-Tuo River Basin based on SWAT model simulations; China. *Sci. Rep.* **2020**, *10*. [[CrossRef](#)]
29. Yan, X.M.; Lu, W.X.; An, Y.K.; Chang, Z.B. Uncertainty analysis of parameters in non-point source pollution simulation: Case study of the application of the Soil and Water Assessment Tool model to Yitong River watershed in northeast China. *Water. Environ. J.* **2019**, *33*, 390–400. [[CrossRef](#)]
30. Tian, P.; Zhang, C. Simulation analysis of jiujiang river basin runoff based on swat model. *IOP Conf. Ser. Earth Environ. Sci.* **2017**, *64*, 012005. [[CrossRef](#)]
31. Jones, R.N.; Chiew, F.H.S.; Boughton, W.C.; Zhang, L. Estimating the sensitivity of mean annual runoff to climate change using selected hydrological models. *Adv. Water. Resour.* **2006**, *29*, 1419–1429. [[CrossRef](#)]
32. Abbaspour, K.C. *User Manual for SWAT-CUP, SWAT Calibration and Uncertainty Analysis Programs*; Swiss Federal Institute of Aquatic Science and Technology, Eawag: Duebendorf, Switzerland, 2007; Volume 93.
33. Savage, M.J.; Thavhana, M.P.; Moeletsi, M.E. SWAT model uncertainty analysis; calibration and validation for runoff simulation in the Luvuvhu River catchment; South Africa. *Phys. Chem. Earth* **2018**, *105*, 115–124. [[CrossRef](#)]
34. Liew, M.W.; Garbrecht, J. Hydrologic simulation of the little Washita River experimental watershed using SWAT. *J. Am. Water. Resour. Assoc.* **2003**, *39*, 14. [[CrossRef](#)]
35. Moriasi, D.; Arnold, J.; Liew, M.W.V.; Bingner, R.L.; Harmel, R.D.; Veith, T.L. Model evaluation guidelines for systematic quantification of accuracy in watershed simulations. *Trans. ASABE* **2007**, *50*, 885–899. [[CrossRef](#)]
36. Jia, X.Q.; Fu, B.J.; Feng, X.M.; Hou, G.H.; Liu, Y.; Wang, X.F. The tradeoff and synergy between ecosystem services in the grain-for-green areas in Northern Shaanxi, China. *Ecol. Indic.* **2014**, *43*, 103–113. [[CrossRef](#)]
37. Yang, Z.Y.; Yu, Y.D.; Wang, J.H.; Yan, D.H. Climate change and its impact on water resources in Yixun River basin. *Adv. Water Sci.* **2011**, *22*, 175–181. [[CrossRef](#)]
38. Gao, J.; Li, F.; Gao, H.; Zhou, C.B.; Zhang, X.L. The impact of land-use change on water-related ecosystem services: A study of the Guishui River Basin, Beijing, China. *J. Clean. Prod.* **2016**. [[CrossRef](#)]
39. Deng, X.Z.; Jiang, Q.O.; Zhan, J.Y.; He, J.Y.; Lin, Y.Z. Simulation on the dynamics of forest area changes in Northeast China. *J. Geogr. Sci.* **2010**, *20*. [[CrossRef](#)]
40. Wen, X.; Deng, X.Z.; Zhang, F. Scale effects of vegetation restoration on soil and water conservation in a semi-arid region in China: Resources conservation and sustainable management. *Resour. Conserv. Recycl.* **2019**, *151*. [[CrossRef](#)]
41. Borjesson, P.; Tufvesson, L.M. Agricultural crop-based biofuels-resource efficiency and environmental performance including direct land use changes. *J. Clean. Prod.* **2011**, *19*, 108–120. [[CrossRef](#)]
42. Gong, H.L.; Yun, P.; Xu, Y.X. Spatio-temporal variation of groundwater recharge in response to variability in precipitation, land use and soil in Yanqing Basin, Beijing, China. *Hydrogeol. J.* **2012**, *20*. [[CrossRef](#)]

43. Guo, B.B.; Zhang, J.; Gong, H.L.; Cheng, X.G. Future climate change impacts on the ecohydrology of Guishui River Basin, China. *Ecolhydrol. Hydrobiol.* **2014**, *14*. [[CrossRef](#)]
44. Kato, Y.; Okami, M.; Katsura, K. Yield potential and water use efficiency of aerobic rice (*Oryza sativa* L.) in Japan. *Field Crops Res.* **2009**, *113*, 328–334. [[CrossRef](#)]
45. Liao, N.; Gu, X.C.; Wang, Y.J.; Xu, H.L.; Fan, Z.L. Analyzing Macro-Level Ecological Change and Micro-Level Farmer Behavior in Manas River Basin, China. *Land* **2020**, *9*, 250. [[CrossRef](#)]
46. Wang, C.L.; Jiang, Q.O.; Shao, Y.Q.; Sun, S.Y.; Xiao, L.; Guo, J.B. Ecological environment assessment based on land use simulation: A case study in the Heihe River Basin. *Sci. Total Environ.* **2019**, 697. [[CrossRef](#)]
47. Oziransky, Y.; Kalmakova, A.G.; Margolina, I.L. Integrated scarce water resource management for a sustainable water supply in arid regions (the experience of the state of Israel). *Arid Ecosyst* **2014**, *4*, 270–276. [[CrossRef](#)]
48. Dragonetti, G.; Khadra, R.; Daccache, A.; Oubelkacem, A.; Choukrallah, R.; Lamaddalena, N. Development and application of a predictive model for treated wastewater irrigation management in a semi-arid area. *Integr. Environ. Assess. Manag.* **2020**. [[CrossRef](#)]
49. Li, J.S.; Fei, L.J.; Li, S.; Xue, C.; Shi, Z.X.; Hinkelmann, R. Development of “water-suitable” agriculture based on a statistical analysis of factors affecting irrigation water demand. *Sci. Total Environ.* **2020**, 744. [[CrossRef](#)]



© 2020 by the authors. Licensee MDPI, Basel, Switzerland. This article is an open access article distributed under the terms and conditions of the Creative Commons Attribution (CC BY) license (<http://creativecommons.org/licenses/by/4.0/>).